DIFFUSION OF H$_2$O IN SMECTITE GELS: OBSTRUCTION EFFECTS OF BOUND H$_2$O LAYERS

Yoshito Nakashima*

Exploration Geophysics Research Group, National Institute of Advanced Industrial Science and Technology, Central 7, Higashi 1-1-1, Tsukuba, Ibaraki 305-8567, Japan

Abstract—In water-rich smectite gels, bound or less mobile H$_2$O layers exist near negatively-charged clay platelets. These bound H$_2$O layers are obstacles to the diffusion of unbound H$_2$O molecules in the pore-space, and therefore reduce the H$_2$O self-diffusion coefficient, D, in the gel system as a whole. In this study, the self-diffusion coefficients of H$_2$O molecules in water-rich gels of Na-rich smectites (montmorillonite, stevensite and hectorite) were measured by pulsed-gradient spin-echo proton nuclear magnetic resonance (NMR) to evaluate the effects of obstruction on D. The NMR results were interpreted using random-walk computer simulations which show that unbound H$_2$O diffuses in the gels while avoiding randomly-placed obstacles (clay platelets sandwiched in immobilized bound H$_2$O layers). A ratio (volume of the clay platelets and immobilized H$_2$O layers)/(volume of clay platelets) was estimated for each water-rich gel. The results showed that the ratio was 8.92, 16.9, 3.32, 3.73 and 3.92 for Wyoming montmorillonite ($\leqslant$5.74 wt.% clay), Tsukinuno montmorillonite ($\leqslant$3.73 wt.% clay), synthetic stevensite ($\leqslant$8.97 wt.% clay), and two synthetic hectorite samples ($\leqslant$11.0 wt.% clay), respectively. The ratios suggest that the thickness of the immobilized H$_2$O layers in the gels is 4.0, 8.0, 1.2, 1.4 and 1.5 nm, respectively, assuming that each clay particle in the gels consists of a single 1 nm-thick platelet. The present study confirmed that the obstruction effects of immobilized H$_2$O layers near the clay surfaces are important in restricting the self-diffusion of unbound H$_2$O in water-rich smectite gels.

Key Words—Hectorite, Montmorillonite, Porous Media, Random Walk, Stevensite, Water.

INTRODUCTION

Groundwater migrates in less permeable clay-rich strata with small Péclet values by pore-volume diffusion or random-walk processes. Consequently, the self-diffusion coefficients of H$_2$O in clay gels, D, are important transport properties in groundwater hydrology (*e.g.* Yu and Neretnieks, 1997). Recent studies revealed that the normalized H$_2$O self-diffusion coefficients, D/D_0, in dilute gels obey simple temperature-independent equations:

$$\ln\left(\frac{D}{D_0}\right) = \alpha[\exp(-\beta w) - 1] \text{ for montmorillonite (1)}$$

and

$$\frac{D}{D_0} = \exp(-\alpha' w) \quad \text{for stevensite and hectorite (2)}$$

where α, β and α' are dimensionless constants, w is the clay weight fraction of the gel (wt.%), and D_0 is the H$_2$O self-diffusion coefficient in bulk water (Nakashima, 2000, 2001a, 2002a,b). Equations 1 and 2 are useful for predicting D in water-rich clay gels at arbitrary temperatures and with arbitrary clay fractions. However, these equations are no more than phenomenological, and no explanation was made for the variation of α, β and α' values between different clay species. The purpose of

the present study is to provide a physical explanation for the dependence of D/D_0 on w. The explanation is based on a hypothesis that bound or less mobile H$_2$O layers near clay surfaces act as obstacles to diffusing unbound H$_2$O molecules, and thereby decrease D/D_0 as w increases (Duval *et al.*, 1999, 2001; Nakashima, 2001b, 2002c). A diffusion model was introduced to discuss the effects of bound H$_2$O layers on D/D_0. Pulsed-gradient spin-echo nuclear magnetic resonance (PGSE NMR) experiments were performed on three different smectites (montmorillonite, stevensite and hectorite) to provide experimental data on D/D_0 as a function of w. Computer simulations of the random walk in porous gels were carried out to investigate the effects of the obstacle volume-fraction on D/D_0. Finally, the results of the PGSE NMR experiments and numerical simulations were combined to elucidate the obstruction effects of bound H$_2$O layers on D/D_0.

MODEL OF H$_2$O DIFFUSION IN CLAY GELS

A model of the H$_2$O diffusion in clay gels is introduced to discuss the effects of bound H$_2$O layers on the H$_2$O self-diffusion in the gels (Figure 1). Free or unbound H$_2$O molecules diffuse in the clay gels by avoiding randomly-placed clay platelets (*e.g.* Figure 7 of Nakashima, 2002d). Here the term 'platelet' refers to a clay particle composed of a single unit of the clay structure (*e.g.* one octahedral sheet and two tetrahedral sheets for smectite). Because the principal exchangeable

* E-mail address of corresponding author:
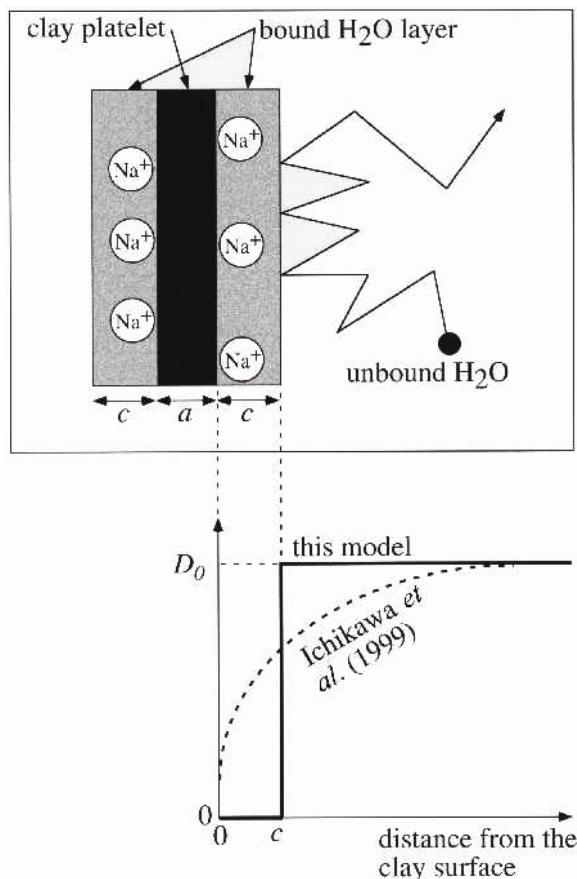nakashima.yoshito@aist .go.jp

9

Figure 1. Model of H_2O self-diffusion in a clay gel. A clay platelet (thickness a) is sandwiched between bound H_2O layers (thickness c). An unbound H_2O molecule (solid circle) in the gel diffuses by avoiding the obstacle (hydrated clay platelets). Counter ions (Na^+) are embedded in the bound H_2O layers. The schematic self-diffusion coefficient (D) profiles simulated by Ichikawa *et al.* (1999) and used in the present study are indicated.

cation is Na^+ for all smectite samples examined, there are Na^+ ions in the gel system to compensate the negative charge of the platelets. Bound H_2O layers several nm thick lie near the negatively charged clay platelets (Ichikawa *et al.*, 1999, 2001). These bound H_2O layers are characterized by a low self-diffusivity compared to that of unbound H_2O far from the clay surfaces. Thus the less mobile H_2O layers increase the apparent volume of the platelets acting as obstacles to diffusion. The unbound H_2O molecules diffuse by avoiding the platelets with bound H_2O layers, and their random-walk trajectories are restricted by the obstacles (platelet plus bound H_2O layers). This apparent volume increase leads to the reduction of D/D_0 for unbound H_2O (Duval *et al.*, 1999). The real D profile near the clay surfaces is continuous as suggested by Ichikawa *et al.* (1999). To make the obstacle size more definite in extent, this continuous D profile was converted to a discrete distribution, and H_2O molecules within the

bound H_2O layers were assumed to be completely immobile (*i.e.* $D = 0$ m²/s) in the model (Figure 1). This discrete-distribution approximation is for estimating the thickness of the bound H_2O layers, and does not influence the D values obtained by the PGSE NMR experiments.

As stated above, unbound H_2O molecules diffuse around the obstacles (platelets with immobilized H_2O layers), and therefore D decreases as the thickness, c, of the immobilized H_2O layers increases. The obstruction effect of the immobilized H_2O layers is defined by

$$\chi = \frac{\phi_{obst}}{\phi_{clay}} \qquad (3)$$

where ϕ_{obst} is the volume fraction of clay platelets plus immobilized H_2O layers, and ϕ_{clay} is that of clay platelets. The χ value is a measure of how strongly the negatively charged clay surfaces attract H_2O molecules. The thickness of the immobilized H_2O layers increases with increasing χ value. If χ is unity, there is no bound H_2O layer near the clay surfaces. The purpose of the present study is to estimate the χ values for water-rich smectite gels.

PGSE NMR EXPERIMENTS

The dependence of D/D_0 on w for smectite gels was measured by PGSE proton NMR to provide the model illustrated in Figure 1 with experimental data. Five Na-rich smectite clays were chosen: two montmorillonite, one stevensite, and two hectorite samples. The Wyoming montmorillonite (SWy-2) is a reference sample of The Clay Minerals Society (http://cms.lanl.gov/). The chemical/mineral composition is given by Mermut and Cano (2001) and Chipera and Bish (2001). The cation exchange capacity (CEC) is 85 meq/100 g (Borden and Giese, 2001). The Tsukinuno montmorillonite is a reference sample (JCSS3101) from The Japan Clay Science Society (http://wwwsoc.nii.ac.jp/cssj2/index.html); its chemical/mineral composition was described by Nakashima *et al.* (1999) and Nakashima (2001a). The average radius, r_{clay}, of the discoidal platelets dispersed in a dilute clay suspension is 400 nm (Monma *et al.*, 1997) and the CEC value is 119 meq/100 g. The stevensite sample is a synthetic Na-rich clay, smecton ST®, obtained from Kunimine Industries Co. Ltd. (http://www.kunimine.co.jp/). The CEC value is 54 meq/100 g and r_{clay} is 21 nm. The chemical composition was described by Nakashima (2002b). One Na-rich hectorite sample used is the synthetic clay, SWN®, by CO-OP Chemical Co., Ltd. (http://www.jade.dti.ne.jp/~coopchem/). The distribution of the radius of the discoidal platelets is bimodal (28 and 140 nm), and the methylene blue capacity (MBC) is 101 meq/100 g (Furusawa, 1997). The chemical composition is as follows: SiO_2 50.99, Al_2O_3 0.03, MgO 24.48,

CaO 0.04, Na$_2$O 3.57, K$_2$O 0.05, H$_2$O 16.03, Li$_2$O 1.30, CO$_2$ 0.85, SO$_3$ 0.09 (total 97.43 wt.%). The other is the synthetic clay, smecton HE®, obtained from Kunimine Industries Co. Ltd. Its chemical composition was given by Nakashima (2000). The MBC value is 126 meq/100 g and r_{clay} is 27 nm. All five clay samples contain interlayer H$_2$O, and the weight loss of each clay powder at 110°C was 4.2, 7.5, 9.9, 8.3 and 8.5 wt.% for SWy-2, Tsukinuno montmorillonite, smecton ST®, SWN®, and smecton HE®, respectively. Because w is the weight fraction of the clay platelets without interlayer H$_2$O, this pre-existing H$_2$O was corrected in the calculation of w.

Although bound H$_2$O molecules exist on the platelet edges in the real clay gels, they are ignored in the model in Figure 1. The volume of the bound H$_2$O on an edge of a single discoidal platelet (platelet radius r_{clay}, thickness a) is $2\pi r_{clay}ac$; that of the H$_2$O bound on the basal surfaces is $2\pi r_{clay}^2 c$. Assuming a reasonable value of $a = 1$ nm, the ratio $2\pi r_{clay}ac/2\pi r_{clay}^2 c = a/r_{clay}$ is as small as, e.g. 1/21 ≈ 5% for stevensite and 1/400 ≈ 0.3% for Tsukinuno montmorillonite. Thus it is a reasonable approximation that the contribution of the bound H$_2$O on the platelet edges to the χ value is negligible.

Water-rich gel samples were prepared by adding deionized water to the powdered clays. The self-diffusion coefficient of a bulk water sample (deionized water) was also measured. Relaxation times (T_1, spin-lattice relaxation time, and T_2, spin-spin relaxation time) for protons associated with H$_2$O in the gel samples and deionized water were measured. The 90° to 180° pulse separation in the T_2 measurements was 0.2 ms for the two montmorillonite samples and 0.5 ms for other clay samples. The bulk densities, ρ_{bulk}, of the gel samples were obtained by weighing samples of known volume. Published diffusion data obtained by PGSE NMR exist for the Tsukinuno montmorillonite and stevensite samples (Nakashima, 2001a, 2002b), but the number of the data points is too small to usefully apply those data to the model of Figure 1. Thus, several water-rich gel samples of the Tsukinuno montmorillonite and stevensite were measured as part of the present study. No PGSE NMR experiments were performed for the smecton HE® gels because extensive NMR data were published by Nakashima (2000).

The H$_2$O self-diffusion coefficients, D, were calculated by measuring the decrease in NMR signal intensity with increasing magnetic field gradients (Stejskal and Tanner, 1965). This PGSE NMR technique was used because it permits non-destructive, fast, precise measurements (e.g. Fripiat et al., 1984; Grandjean and Laszlo, 1989; Nakashima, 2000). The NMR spin-echo signal intensity, I, is given by:

$$I/I_0 = \exp(-bD) \qquad (4)$$

where

$$b = (\gamma G\delta)^2(\Delta - \delta/3) \qquad (5)$$

The quantity I_0 is the signal intensity without pulsed field gradients, γ is the gyromagnetic ratio of a proton (2.675×10^8 rad/Ts), G is the strength of the gradient pulses, δ is the duration of the field gradient pulses, and Δ is the interval between two gradient pulses (e.g. Johnson, 1996).

The PGSE NMR measurements were performed with a NMS120 proton spectrometer (Bruker, Karlsruhe, Germany) at a resonant frequency of 20 MHz. Each 1 cm^3 sample was placed in a separate 10 mm external diameter glass tube. The pulse parameters were as follows: $\delta = 0.7$ ms, echo time $T_E = 28$ ms, $\Delta = 14$ ms, and 16 echo signals were stacked. For the SWy-2 gel samples ($w \geqslant 18.2$ wt.%) alone, δ, T_E, and Δ were taken to be 1.2, 8 and 4 ms, respectively, because of the short T_2 values of the water-poor Fe-rich samples. In preliminary experiments, the independence of D from Δ values ($\Delta = 14$–210 ms) was confirmed for some gel samples to ensure that the samples were in the restricted diffusion regime (e.g. Nakashima, 2000, 2001a). The repetition time of the pulse sequence, T_R, was set to $T_R = 5T_1$ to meet the full relaxation condition. About eight values of G (from 0 to 2.1 T/m) were used for each specific clay fraction and temperature to measure the dependence of I/I_0 on b. D was then calculated by performing a regression analysis of the data sets (I/I_0 vs. b) combining equations 4 and 5. The experiments were performed at atmospheric pressure and therefore no pressure vessel was used. Results from four or five temperatures were used to calculate the activation energy of the diffusion process. The activation energy, E, is calculated via the equation

$$D = A\exp\left(-\frac{E}{RT}\right) \qquad (6)$$

where A is a constant, R is the gas constant, and T is the absolute temperature.

To probe the structure (tortuosity) of porous media accurately in diffusion experiments, the diffusion distance must be larger than the characteristic size of the pore structure (e.g. Latour et al., 1995). The characteristic diffusion distance of H$_2$O molecules (root-mean-square displacement of the random walker) measured by PGSE NMR is $(6D\Delta)^{1/2}$ (e.g. Callaghan, 1991). Substituting typical values for D and Δ (2×10^{-9} m^2/s and 14 ms, respectively), $(6D\Delta)^{1/2}$ is calculated to be 13 μm. This value is much larger than the sub-micrometer clay gel pore size, and therefore the PGSE NMR technique used here is capable of probing the clay gel structure correctly.

COMPUTER SIMULATIONS OF A RANDOM WALK

Numerical simulations of diffusion in random porous media were also performed to relate D/D_0 to ϕ_{obst}. The random porous media are the model of the water-rich clay gels. In the model, point obstacles (platelets and

immobilized H_2O layers) are placed randomly in a three-dimensional discrete lattice, and the walker migrates by a lattice walk while avoiding the obstacles. It is a reasonable approximation that the obstacles are point-like because the diffusion distance measured by NMR, $(6D\Delta)^{1/2} \approx 13$ μm, is much larger than the clay grain size (*e.g.* $r_{clay} = 21$ nm for smecton ST$^®$). The purpose of the simulations is to obtain the quantitative dependence of D/D_0 on ϕ_{obst}.

A public-domain program, RW3D.m, developed by Watanabe and Nakashima (2002) was used for the random-walk simulations in the random porous media. The random porous media are the discrete system composed of a three-dimensional simple cubic lattice (the lattice constant is unity) with $300 \times 300 \times 300$ volume elements (voxels). Randomly selected voxels are occupied by obstacles, such that the fraction of the occupied voxels is ϕ_{obst}. Random walkers migrate via discrete voxels throughout the lattice corresponding to a pore space. At the beginning of the lattice walk (*i.e.* $\tau = 0$ where τ is dimensionless integer time or step number in the lattice walk), the walker is located near the center of the three-dimensional system. The walker executes a random jump to one of the six nearest unoccupied voxels, and τ is incremented by unit time after the jump ($\tau + 1$). If the randomly selected voxel is occupied by an obstacle, the time is incremented but the jump is not performed.

The calculation of D/D_0 was performed as follows. The mean-square displacement of the random walkers, $<r^2>$, is

$$<r(\tau)^2> = \frac{1}{n}\sum_{i=1}^{n} r_i(\tau)^2 \qquad (7)$$

where n is the number of runs of the random walk, and $r_i(\tau)$ is the distance between the walker's position at time τ and that at $\tau = 0$ for the *i*th run. The diffusion coefficient, D, is given by the time derivative of $<r^2>$ (*e.g.* Chang *et al.*, 1998). Therefore, the normalized diffusion coefficient, D/D_0, is calculated by

$$\frac{D}{D_0} = \frac{\left(\frac{d<r(\tau)^2>}{d\tau}\right)}{\left(\frac{d<r(\tau)^2>}{d\tau}\right)_{\phi_{obst}=0}} \qquad (8)$$

The exact solution for the lattice walk in free space (*i.e.* $\phi_{obst} = 0$ vol.%) is $<r^2> = \tau$ if the lattice constant is unity (*e.g.* Stauffer, 1985). Thus the denominator of the right hand side of equation 8 is unity. Random walk simulations for various ϕ_{obst} were performed, and D/D_0 was obtained as a function of ϕ_{obst}.

RESULTS

PGSE NMR experiments

Examples of *b*-dependent spin-echo intensities are shown for selected SWy-2 gel samples in Figure 2. The parameters, δ and Δ, were fixed in the experiments, and

the *b* value was changed by choosing some *G* values systematically. The variation in the spin-echo signal with the strength of the magnetic field gradient can be clearly seen. The slope of each regression line represents the negative value of the self-diffusion coefficient of H_2O, D.

All results of the NMR experiments are listed in Tables 1–4. The data on D_0 (*i.e.* D at $w = 0$ wt.%) in Tables 1 and 4 agree well with the literature (Mills, 1973). The results of these bulk-water experiments suggest that the accuracy of the PGSE NMR experiments is approximately 10^{-11} m²/s. The H_2O self-diffusion coefficients, D, in SWy-2 and SWN$^®$ gels are shown graphically in Figures 3 and 4. Figures 3a and 4a reveal that α, β and α' are nearly independent of sample temperature. As a result, temperature-independent master curves (equations 1 and 2) could be determined easily (Figures 3b, 4b). Arrhenius plots of the diffusion data are shown in Figures 3c and 4c, and the corresponding activation energies, E, calculated using equation 6 are listed in Tables 1 and 4. The activation energies of bulk water (17.4 kJ/mol for 30.1–60.8°C in Table 1, 18.4 kJ/mol for 20.1–60.7°C in Table 4) are nearly equal to the results reported by Mills (1973) of 17.6 kJ/mol for the temperature range 15–45°C, suggesting that the NMR experiments were performed in a reliable manner. Tables 1 and 4 indicate that the activation energy for each gel sample nearly equals the value for bulk water. The temperature independence of α, β and α' in Figures 3a and 4a is a consequence of this w independence of E.
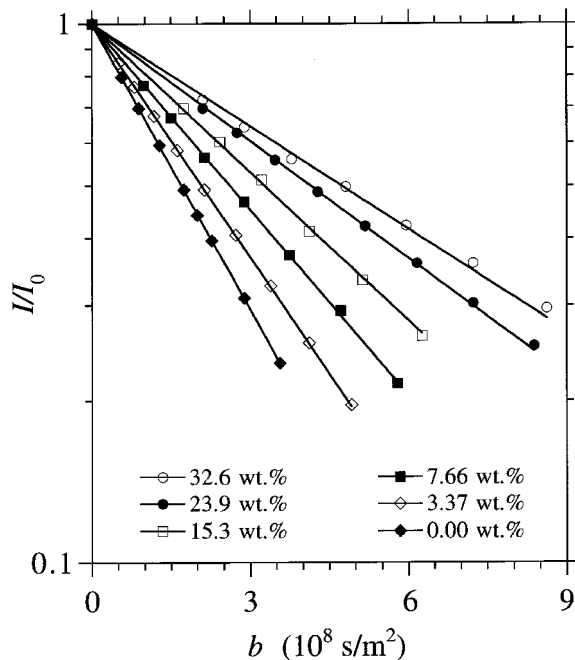

Figure 2. NMR-signal intensities *vs.* *b* factor for six SWy-2 gel samples at 50.5°C. Each clay fraction (*w*) is indicated. The data points were fitted to equation 4 by a least-squares method.

Table 1. Results of the NMR experiments on SWy-2 montmorillonite gels.

w	ρ_{bulk} 22°C	T_1 39.8°C	T_2 39.8°C	D 30.1°C	D 39.8°C	D 50.5°C	D 60.8°C	E	Δ
(wt.%)	(g/mL)	(ms)	(ms)	- - - - - - - - - (10^{-9} m^2/s) - - - - - - - - -				(kJ/mol)	(ms)
0.00	1.0	3850	3470	2.56	3.26	4.07	4.96	17.4	14
1.33	1.0	340	248	2.36	2.97	3.74	4.58	17.6	14
2.16	1.0	212	135	2.26	2.91	3.59	4.37	17.6	14
2.44	1.0	186	129	2.23	2.83	3.53	4.31	17.4	14
2.87	1.0	162	103	2.13	2.71	3.38	4.14	17.5	14
3.37	1.0	128	87.5	2.09	2.64	3.32	4.06	17.6	14
3.88	1.0	116	75.5	1.99	2.55	3.18	3.89	17.7	14
4.37	1.0	97.3	65.0	1.97	2.50	3.12	3.81	17.4	14
4.89	1.0	89.2	58.9	1.90	2.42	3.02	3.64	17.5	14
5.74	1.0	76.3	50.0	1.82	2.33	2.88	3.52	17.5	14
7.66	1.1	57.0	37.4	1.67	2.11	2.64	3.20	17.2	14
9.57	1.1	44.6	27.7	1.53	1.94	2.39	2.89	16.8	14
11.5	1.1	36.5	22.4	1.47	1.86	2.30	2.80	17.4	14
13.4	1.1	27.7	19.6	1.35	1.69	2.19	2.67	18.4	14
15.3	1.2	22.6	16.2	1.27	1.61	2.12	2.54	19.0	14
18.2	1.2	18.2	12.8	1.20	1.49	1.90	2.32	17.8	4
21.1	1.2	16.1	11.1	1.13	1.43	1.79	2.18	17.4	4
23.9	1.2	14.3	9.12	1.05	1.34	1.67	2.04	17.8	4
26.8	1.2	12.6	7.86	1.01	1.21	1.51	1.89	17.6	4
29.7	1.3	12.0	6.80	0.978	1.22	1.52	1.83	16.7	4
32.6	1.3	10.9	5.81	0.959	1.16	1.49	1.73	16.3	4
35.4	1.3	8.81	4.69	0.940	1.11	1.48	1.71	17.1	4

Nakashima (2001a) and Nakashima (2002b) found that D for Tsukinuno montmorillonite and stevensite gels obeyed equations 1 and 2, respectively. The additional data listed in Tables 2 and 3 are consistent with this finding. The graphic presentations of D as a function of w and T for these two clay species are omitted because they are similar to those for SWy-2 and SWN® , respectively, except for the difference in the numerical constants (α, β and α').

The values of the numerical constants for Wyoming montmorillonite, $\alpha = 1.21$ and $\beta = 0.0564$ (Figure 3b), are smaller than those for Tsukinuno montmorillonite ($\alpha = 1.77$ and $\beta = 0.0798$; Nakashima, 2001a). The α' value for SWN® hectorite ($\alpha' = 0.0220$ in Figure 4b) is different from that for smecton HE® hectorite ($\alpha' = 0.0257$; Nakashima, 2000) and that for smecton ST® stevensite ($\alpha' = 0.0198$; Nakashima, 2002b). This difference will be explained in a later section in terms of the difference of the χ value or the difference in the thickness of the bound H$_2$O layers.

Random-walk simulations

An example of a random porous medium equivalent to $\phi_{obst} = 0.1$ vol.% is shown in Figure 5a. Figure 5b depicts a random-walk trajectory restricted by the obstacles (platelets with immobilized H$_2$O layers). The obtained mean-square displacement of the random walkers, $<r^2>$, is shown in Figure 5c. Random walks, each of more than 4000 steps, were performed, and $n = 2000$ in the present study. The slope of $<r^2>$ for $\phi_{obst} = 0.0$ vol.% of Figure 5c was estimated to be 1.003 by the linear regression analysis. This value is nearly equal to the theoretically expected value (unity) suggesting that the random-walk simulations were performed in a reliable manner.

The temporal gradients of $<r^2>$ in Figure 5c were calculated using a least-squares method, and D/D_0 was expressed as a function of ϕ_{obst} using equation 8 (Figure 5d). Linear regression analysis applied to the data points of Figure 5d reveals that

$$\frac{D}{D_0} = 1 - 0.0157\,\phi_{obst} \qquad (9)$$

Table 2. Results of the NMR experiments of Tsukinuno montmorillonite gels ($\Delta = 14$ ms).

w	ρ_{bulk} 22°C	T_1 39.8°C	T_2 39.8°C	D 30.4°C	D 39.8°C	D 50.5°C	D 60.0°C	E
(wt.%)	(g/mL)	(ms)	(ms)	- - - - - - - - - - (10^{-9} m^2/s) - - - - - - - - - -				(kJ/mol)
1.30	1.0	446	338	2.16	2.69	3.40	4.11	17.7
2.36	1.0	258	198	1.91	2.39	3.01	3.64	17.8
3.28	1.0	189	142	1.76	2.20	2.79	3.37	17.9
4.26	1.1	144	109	1.62	2.03	2.56	3.09	17.7

Table 3. Results of the NMR experiments of stevensite gels ($\Delta = 14$ ms).

w	ρ_{bulk} 22°C	T_1 39.8°C	T_2 39.8°C	D 20.0°C	D 30.1°C	D 39.8°C	D 50.3°C	D 60.3°C	E
(wt.%)	(g/mL)	(ms)	(ms)						(kJ/mol)
				- - - - - - - - - - - - - (10^{-9} m^2/s) - - - - - - - - - - - - -					
1.01	1.0	3212	701	1.89	2.48	3.13	3.95	4.80	18.6
2.66	1.0	2629	345	1.81	2.39	3.02	3.82	4.63	18.6
4.51	1.1	2195	229	1.75	2.31	2.92	3.67	4.45	18.5
6.33	1.1	1859	171	1.68	2.23	2.82	3.54	4.30	18.5
8.13	1.1	1617	137	1.62	2.15	2.72	3.41	4.14	18.5

The volume fraction of the clay platelet (in vol.%), ϕ_{clay}, can be related to the clay weight fraction (in wt.%), w, by the following equation:

$$\phi_{clay} = \frac{w}{\left(\frac{\rho_{clay}}{\rho_{water}}\right) + \left[1 - \left(\rho_{clay}\right)\right]\frac{w}{100}} \quad (10)$$

where ρ_{clay} and ρ_{water} are the densities of clay grains and bulk water, respectively. Combining equations 3, 9 and 10 gives

$$\frac{D}{D_0} = 1 - 0.0157\frac{\chi w}{\left(\frac{\rho_{clay}}{\rho_{water}}\right) + \left[1 - \left(\rho_{clay}\right)\right]\frac{w}{100}} \quad (11)$$

Equation 11 is the final expression of the effects of χ on the normalized H$_2$O self-diffusion coefficient, D/D_0.

DISCUSSION

The purpose of the present study was to calculate χ values defined by equation 3 for water-rich smectite gels. Equation 11 was applied to the NMR data (Tables 1–4) to obtain χ values for montmorillonite, stevensite and hectorite clays. The thickness of bound H$_2$O layers was also estimated based on an assumed microstructure for the clay gels.

The application of equation 11 to the NMR diffusion data is shown in Figures 6–8. A value of 2.7 was assumed for ρ_{clay}/ρ_{water}. The χ values were determined by fitting equation 11 to the data points with small w values because the fitting is worse for large-w samples. The following data points of small-w samples were chosen to determine χ by a least-squares method: $w \leqslant$ 5.74 wt.% (*i.e.* $\phi_{clay} \leqslant$ 2.21 vol.%) for Wyoming montmorillonite, $w \leqslant$ 3.73 wt.% ($\phi_{clay} \leqslant$ 1.41 vol.%) for Tsukinuno montmorillonite, $w \leqslant$ 8.97 wt.% ($\phi_{clay} \leqslant$ 3.52 vol.%) for stevensite, and $w \leqslant$ 11.0 wt.% ($\phi_{clay} \leqslant$ 4.38 vol.%) for SWN® and smecton HE®. The χ values obtained are listed in Table 5.

Nakashima (2000, 2001a, 2002b) described the phenomenological dependence of D/D_0 on w for montmorillonite, stevensite, and hectorite, but no physical explanation was provided. The dependence of D/D_0 on w was explained successfully in the present study using a

Table 4. Results of the NMR experiments of hectorite (SWN®) gels ($\Delta = 14$ ms).

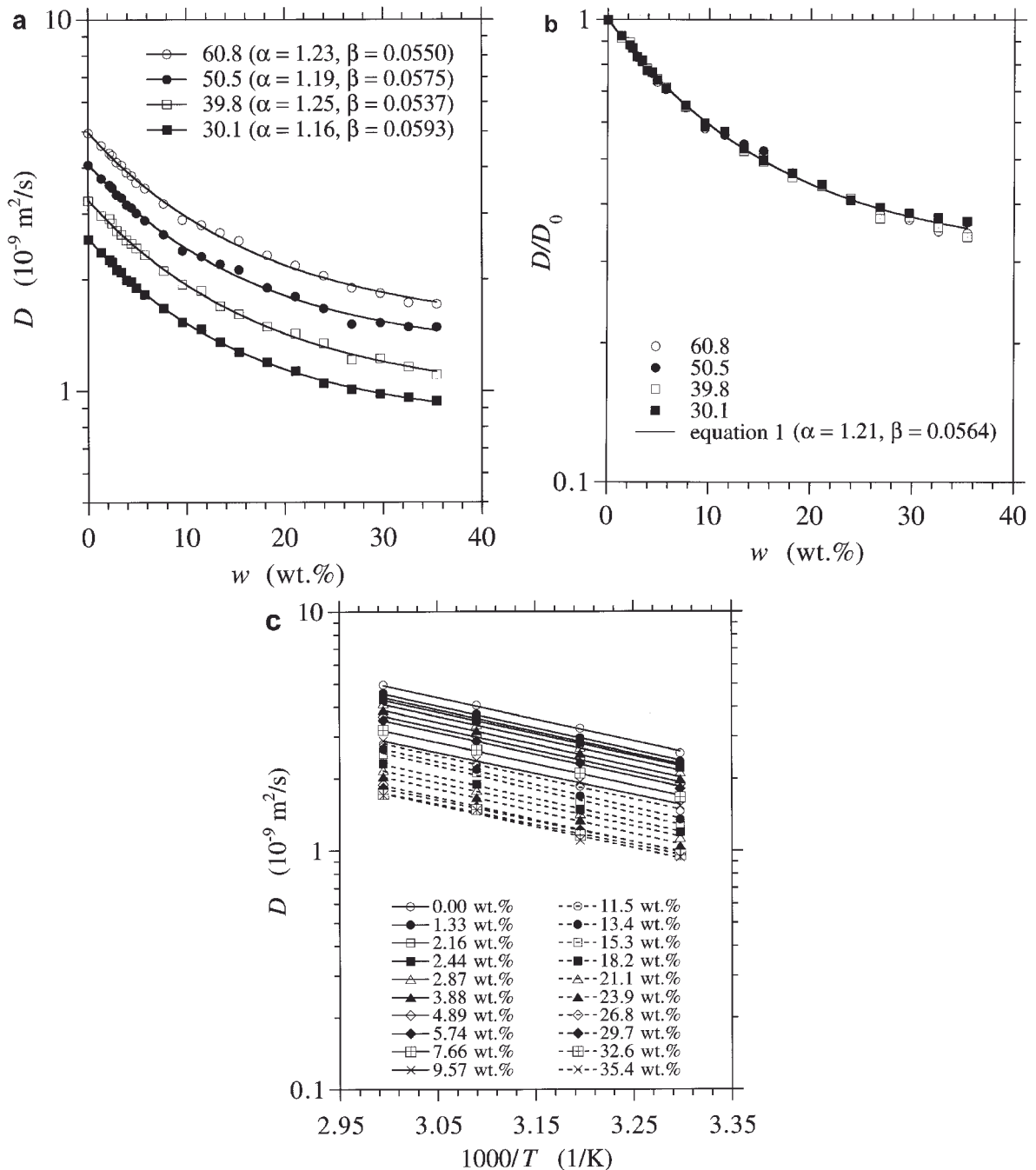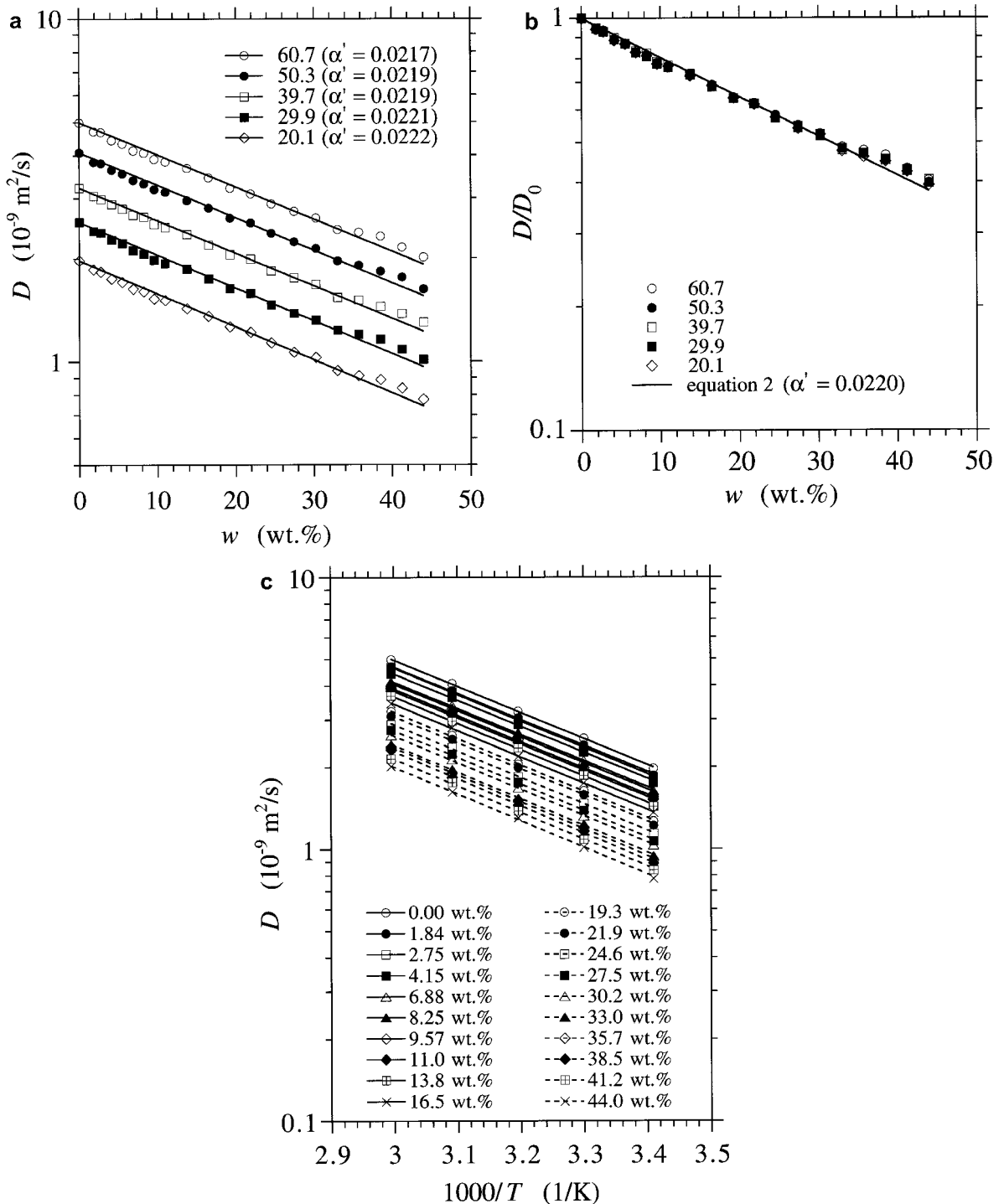| w	ρ_{bulk} 26°C	T_1 39.7°C	T_2 39.7°C	D 20.1°C	D 29.9°C	D 39.7°C	D 50.3°C	D 60.7°C	E
(wt.%)	(g/mL)	(ms)	(ms)						(kJ/mol)
				- - - - - - - - - - - - - (10^{-9} m^2/s) - - - - - - - - - - - - -					
0.00	1.0	3460	3080	1.98	2.56	3.22	4.08	4.99	18.4
1.84	1.0	2708	1025	1.86	2.41	3.05	3.83	4.70	18.4
2.75	1.0	2230	705	1.84	2.38	2.99	3.79	4.68	18.6
4.15	1.1	2107	537	1.75	2.27	2.88	3.63	4.43	18.4
5.50	1.1	1671	420	1.71	2.22	2.80	3.54	4.33	18.4
6.88	1.1	1566	362	1.63	2.11	2.68	3.39	4.13	18.4
8.25	1.1	1325	283	1.61	2.07	2.65	3.31	4.07	18.5
9.57	1.1	1293	268	1.53	1.98	2.53	3.18	3.90	18.6
11.0	1.1	1092	215	1.51	1.94	2.47	3.13	3.83	18.6
13.8	1.1	911	168	1.43	1.87	2.36	2.96	3.67	18.6
16.5	1.2	787	140	1.36	1.75	2.19	2.81	3.44	18.6
19.3	1.2	664	114	1.27	1.64	2.06	2.63	3.21	18.6
21.9	1.2	597	101	1.22	1.58	2.00	2.54	3.09	18.5
24.6	1.2	512	86.9	1.14	1.47	1.84	2.37	2.89	18.6
27.5	1.2	454	71.4	1.07	1.39	1.76	2.24	2.75	18.8
30.2	1.3	403	63.4	1.03	1.32	1.68	2.14	2.63	18.7
33.0	1.3	347	53.1	0.94	1.24	1.54	1.97	2.43	18.8
35.7	1.3	335	51.5	0.91	1.20	1.51	1.91	2.39	19.0
38.5	1.3	312	47.5	0.89	1.16	1.45	1.84	2.32	19.1
41.2	1.4	275	40.3	0.84	1.09	1.38	1.76	2.16	18.8
44.0	1.4	247	36.3	0.78	1.02	1.30	1.63	2.02	18.8

Figure 3. Self-diffusion coefficient of H$_2$O, D, in SWy-2 gels (data from Table 1). (a) Semi-log plot of D as a function of clay fraction (w) at various temperatures (°C). (b) Normalized H$_2$O self-diffusion coefficient, D/D_0, for 30.1, 39.8, 50.5 and 60.8°C. Note that D/D_0 is independent of temperature. (c) Arrhenius plot of D for various clay fractions. Parameters α and β in equation 1 were obtained by a least-squares method for the data shown in (a) and (b). Data points were fitted to equation 6 by a least-squares method for (c).

single physical parameter, χ. All χ values in Table 5 are significantly >2, indicating that the clay platelets attract H$_2$O molecules larger than the volume of the platelets. Thus the obstruction effect of the immobilized-H$_2$O volume is larger than that of the platelets' volume. The present study revealed that the obstruction effect of the immobilized H$_2$O layers near negatively-charged clay surfaces is important in controlling the self-diffusion of unbound H$_2$O.

Nakashima (2000, 2002b) argued that effects of bound H$_2$O on D/D_0 were negligible and D/D_0 was controlled only by the obstruction effect of the platelets.

Figure 4. Self-diffusion coefficient of H_2O, D, in hectorite (SWN®) gels (data from Table 4). (a) Semi-log plot of D as a function of clay fraction, w, at various temperatures (°C). (b) Normalized H_2O self-diffusion coefficient, D/D_0, for 20.1, 29.9, 39.7, 50.3 and 60.7°C. Note that D/D_0 is independent of temperature. (c) Arrhenius plot of D for various clay fractions. The parameter α' in equation 2 was obtained by a least-squares method for the data shown in (a) and (b). Data points were fitted to equation 6 by a least-squares method for (c).

The present study shows that this interpretation is misleading. Clay platelets were approximated by randomly covered circles in the gel model of Nakashima (2000, 2002b). Although the value of the covering density of the circles was critical for the accuracy of the model, the statistical ambiguity of the random covering

Figure 5. Computer simulation of a lattice walk in a random porous medium using the program, RW3D.m. (a) Example of the random porous media. Obstacles (solid points) are randomly placed in the lattice of 300^3 voxels. The number of the obstacles is 27000, and the obstacle volume fraction (ϕ_{obst}) is $27,000/300^3 = 0.1$ vol.%. (b) An example of a random-walk trajectory through the pore-space of the random porous media for a single walker over 6000 time steps ($\phi_{obst} = 19.8$ vol.%). The initial ($\tau = 0$) and final ($\tau = 6000$) positions of the walker are marked by open circles. (c) Mean-square displacement of the random walk averaged over 2000 walkers calculated using equation 7. The value of ϕ_{obst} is indicated. (d) Normalized diffusion coefficient for the random porous media calculated by equation 8. Data are from (c). The slope was found to be 0.0157 using a least-squares method.

computer simulations used to estimate the value was as large as 5−9. This large ambiguity is a possible cause of the misleading argument that $c \ll a$.

Non-clay minerals (*e.g.* quartz) exist within the natural clay samples studied here (SWy-2 and Tsukinuno montmorillonite), and may also act as obstacles to the diffusion of unbound H₂O. However, the contribution of the non-clay minerals to the NMR diffusion data is probably negligible. For example, the SWy-2 powder is composed of ~75% montmorillonite and 25% non-smectite minerals (Chipera and Bish, 2001). Because the χ value of SWy-2 is 8.92, the contribution of the non-clay minerals to the NMR diffusion data is as small as $25/(25 + 75 \times 8.92) \approx 4\%$. A similar calculation for the Tsukinuno montmorillonite sample ($\chi = 16.9$), whose non-clay mineral
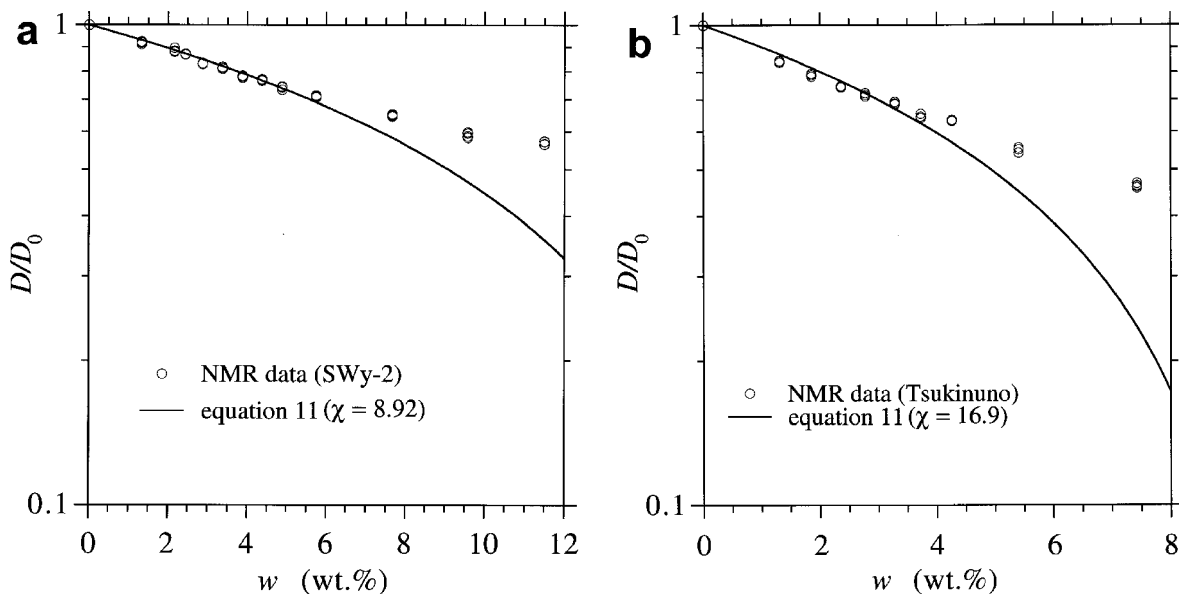
Figure 6. Normalized diffusion coefficients of H_2O, D/D_0, in montmorillonite gels. Equation 11 for the best-fit χ value is also shown. (a) Wyoming montmorillonite (SWy-2) for 30.1–60.8°C. Data from Table 1. (b) Tsukinuno montmorillonite for 30.4–60.0°C. Data from Table 2 and Nakashima (2001b).

Figure 7. Normalized diffusion coefficients of H_2O, D/D_0, in stevensite gels for 20.0–60.3°C. Equation 11 for the best fit χ value is also shown. Data from Table 3 and Nakashima (2002b).

content is ~1%, shows that the contribution is $1/(1 + 99 \times 16.9) \approx 0.06\%$. Thus, the undesirable effect of impurities in the clay samples studied is probably negligible.

The χ values differ between the two montmorillonite and hectorite samples (Table 5). A semi-quantitative explanation for the difference is possible in terms of the layer charge and chemical composition of the clay. The χ value is a measure of how strongly negatively-charged clay surfaces attract H_2O molecules, and therefore increases as the layer charge of the platelet increases. The CEC or MBC can be used as a measure of the layer charge. A molar ratio, Ca/Na, is also an important measure because Na-rich smectites are more expandable and attract more H_2O molecules than Ca-rich smectites. The CEC value is 85 meq/100 g (Borden and Giese, 2001), and Ca/Na = 0.44 (Mermut and Cano, 2001) for SWy-2. The CEC value is 119 meq/100 g and Ca/Na = 0.09 for Tsukinuno montmorillonite. The MBC value is 101 meq/100 g and Ca/Na = 0.01 for SWN®, and MBC value is 126 meq/100 g and Ca/Na = 0.01 for smecton HE®. These values suggest that Tsukinuno montmorillonite and smecton HE® attract more H_2O molecules than SWy-2 and SWN®, respectively. This is consistent with the larger χ values of Tsukinuno montmorillonite and smecton HE® compared with those of SWy-2 and SWN® in Table 5.

The thickness of the bound H_2O layers, c, can be estimated if the number of platelets in a tactoid (aggregate of platelets) is assumed. Although some studies exist (Cebula *et al.*, 1980; Fripiat *et al.*, 1982; Yong, 1999; Suzuki *et al.*, 2001; Kasama *et al.*, 2001), the issue of the number of unit layers forming a tactoid in clay-water systems is controversial and not fully resolved. Thus two simple models are assumed in the present study: platelets are completely dispersed (Figure 9a); two platelets gather to form a tactoid (Figure 9b). The platelets are bound by an immobilized H_2O layer of thickness d in Figure 9b. Counter ions (Na⁺) exist in the bound H_2O layers as shown in Figure 1, but they are omitted in Figure 9. In Figure 9a, χ is related to c by
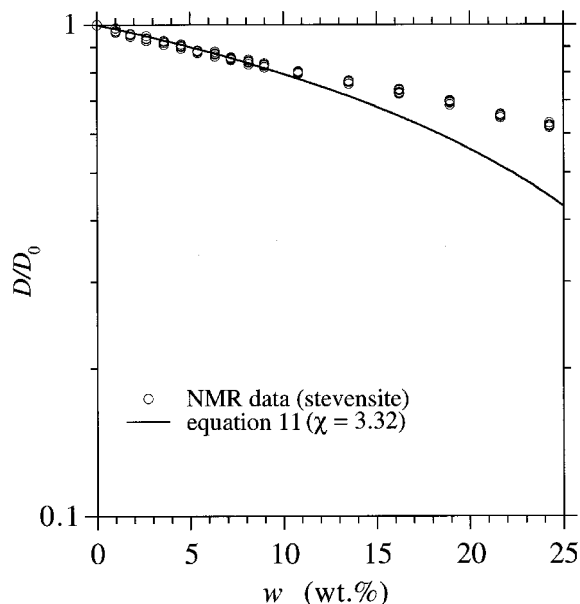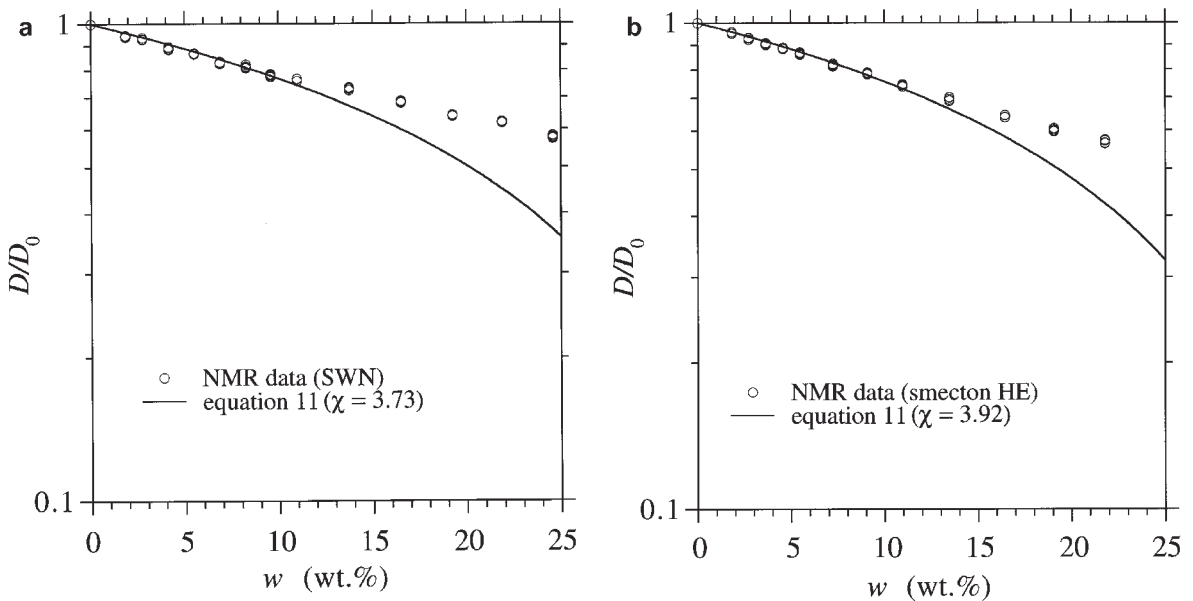
Figure 8. Normalized diffusion coefficients of H$_2$O, D/D_0, in hectorite gels. Equation 11 for the best fit χ-value is also shown. (a) CO-OP SWN® for 20.1–60.7°C. Data from Table 4. (b) Kunimine smecton HE® for 20.0–60.3°C. Data from Nakashima (2000).

$$\chi = (a + 2c)/a \qquad (12)$$

whereas if the clay structure is as shown in Figure 9b, then χ is given by

$$\chi = (2a + 2c + d)/2a \qquad (13)$$

The c values calculated using equations 12 and 13 are listed in Table 5. According to Cebula *et al.* (1980), it is appropriate to assume that $d = 0.4$ nm (the thickness of two molecular layers of H$_2$O) and $a = 1$ nm. Table 5 suggests that the thickness of the bound H$_2$O layers is several nanometers if the platelets are completely dispersed (Figure 9a). Ichikawa *et al.* (1999) suggested using molecular dynamics such that the c value of montmorillonite completely dispersed in water is a few nm. Duval *et al.* (1999, 2001) estimated the c of hectorite to be 1–3 nm. These values from the literature are approximately equal to those listed in Table 5 suggesting that the methods employed in the present study are reasonable.

Counterions (Na$^+$) exist in the gel system (Figure 1), and attract H$_2$O molecules to form hydrated ions.

However, the obstruction effect of the hydrated Na$^+$ ions on the self-diffusivity of unbound H$_2$O is negligible. In aqueous solutions, some H$_2$O molecules are bound to each Na$^+$ ion, and stay in the first hydration shell at a residence time of ~10 ps (Ohtaki and Radnai, 1993). The hydrated radius of the Na$^+$ ion is 0.299 nm (*e.g.* Zhou *et al.*, 2002), and therefore the volume of the spherical hydrated Na$^+$ ions is 6.7×10^{-5} cm^3/mol. These hydrated Na$^+$ ions are possible obstacles to the self-diffusion of unbound H$_2$O if Na$^+$ ions are located outside the bound H$_2$O layers formed by the platelets. However, a molecular dynamics simulation study by Ichikawa *et al.* (1999) suggested that Na$^+$ ions are completely embedded within the bound H$_2$O layers of the clay surfaces (Figure 1). Thus there is no need to add the obstruction effect of hydrated Na$^+$ ions to equation 11. It is possible to calculate the volumes of hydrated Na$^+$ ions and of bound H$_2$O layers using the data for w, ϕ_{clay}, χ, ρ_{bulk}, and CEC or MBC. For example, the total volume of spherical hydrated Na$^+$ ions is $6.7 \times 10^{-5} \times$ CEC $\times w/10 = 0.0032$ cm^3, and that of bound H$_2$O layers formed by the negatively charged platelets is

Table 5. The χ and c values for water-rich smectite gels. χ is from Figures 6–8. c was calculated for two microstructure models (Figure 9a,b) using equation 12 or 13 ($a = 1.0$ nm and $d = 0.4$ nm).

Clay	χ	c (nm) for Figure 9a	c (nm) for Figure 9b
SWy-2 montmorillonite	8.92	4.0	7.7
Tsukinuno montmorillonite	16.9	8.0	15.7
Stevensite	3.32	1.2	2.1
SWN® hectorite	3.73	1.4	2.5
Smecton HE® hectorite	3.92	1.5	2.7

$\chi\phi_{clay}/100\rho_{bulk} = 0.11$ cm^3 for a stevensite gel sample of 1.0 g ($w = 8.97$ wt.%). Thus the volume fraction of hydrated Na$^+$ ions embedded in the bound H$_2$O layers of platelets is as small as $0.0032/0.11 = 3\%$. Small volume-fraction values of several percent or less were also obtained for different w values and clay species. These calculations suggest that the contribution of hydrated Na$^+$ ions to the obstruction effect is negligible.

Figures 6–8 show that the discrepancy between the NMR data and equation 11 occurs for large-w samples (*e.g.* $w > 6$ wt.% in Figure 6a). There are some possible explanations for the discrepancy. One possible explanation is related to the breakdown of the random porous media model. Equation 11 was derived by assuming the random porous media (Figure 5a). In dense or large-w gels, the clay particles are not randomly placed but form an ordered structure (*e.g.* Yong, 1999). This ordered structure (*e.g.* card-house structure) probably forms percolation clusters of pore-space through which unbound H$_2$O molecules can diffuse easily. This is a possible reason for the underestimation by equation 11 for large w. An advanced diffusion model assuming the ordered arrangement of clay particles (*e.g.* Suzuki *et al.*, 2001) is needed to discuss the H$_2$O diffusion in large-w clay gels.

Another possible explanation for the discrepancy is the decrease of the χ value for large-w samples. The χ values in Table 5 were derived by assuming that they are w-independent, which implies that the microstructure (number of platelets in a tactoid) is also w-independent. As a result, the fitting of equation 11 was restricted to the data points of small w in Figures 6–8. However, all NMR data points in Figures 6–8 can be fitted by equation 11 if w-dependent χ values are assumed. For example, equation 11 can be fitted to the data points for $w \geqslant 7.66$ wt.% in Figure 6a if a χ value of <8.92 is assumed. The decreasing χ value with increasing w suggests that the obstruction volume per platelet decreases for large-w samples. Kasama *et al.* (2001) argued that platelets collect to form tactoids or aggregates in gels of large w. The spacing, d, between platelets in tactoids (*e.g.* 0.4 nm; Cebula *et al.*, 1980) is smaller than c values (Table 5) calculated for a completely dispersed system (Figure 9a). This implies that the volume of the bound H$_2$O layers is reduced if completely dispersed platelets collect to form aggregates. Thus the increasing fraction of aggregates in large-w gels is a possible cause for the decrease of χ value. Further studies on the w-dependent tactoid-thickness distribution of clay gels are needed to test this explanation.
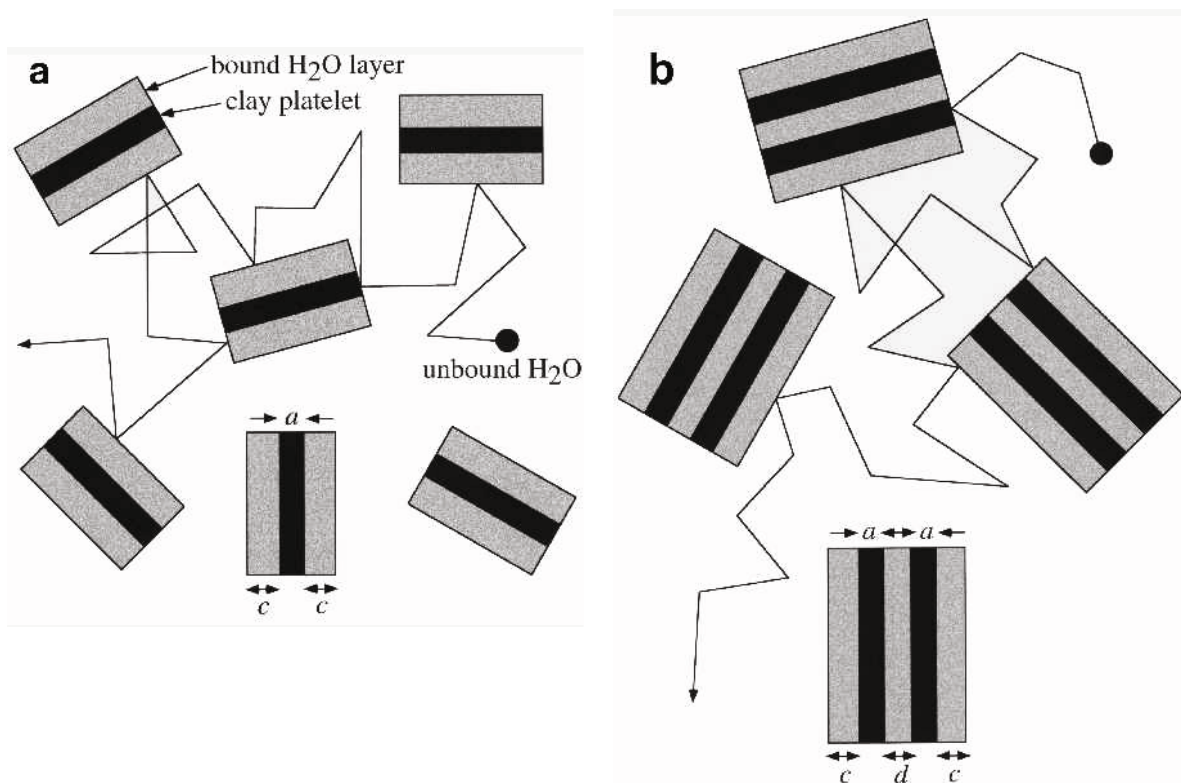

Figure 9. Examples of possible microstructures of clay gels. The diffusing unbound H$_2$O molecule goes around the hydrated clay particles, and the H$_2$O self-diffusion coefficient is reduced by the tortuous structure of the gel. (a) Each clay particle consists of a single clay platelet (thickness a) sandwiched between bound H$_2$O layers (thickness c). (b) Each clay particle consists of two clay platelets interleaved with a bound H$_2$O layer (thickness d).

CONCLUSIONS

The present study revealed that the dependence of D/D_0 on w for water-rich smectite gels can be explained by a model (Figure 9) in which unbound H_2O molecules diffuse by avoiding randomly-placed clay platelets sandwiched in immobilized H_2O layers. Diffusion measurements of other [1]H-bearing materials (*e.g.* glycerin; Tokita *et al.*, 1996) and nuclei (*e.g.* [23]Na; Feinauer and Majer, 2001) are also possible using PGSE NMR techniques. Thus PGSE NMR experiments combined with random-walk simulations of a microstructural model are useful for studying material diffusion in clay gels.

REFERENCES

Borden, D. and Giese, R.F. (2001) Baseline studies of the Clay Minerals Society source clays: Cation exchange capacity measurements by the ammonia-electrode method. *Clays and Clay Minerals*, **49**, 444–445.

Callaghan, P.T. (1991) *Principles of Nuclear Magnetic Resonance Microscopy*. Oxford University Press, Oxford, UK, 492 pp.

Cebula, D.J., Thomas, R.K. and White, J.W. (1980) Small angle neutron scattering from dilute aqueous dispersions of clay. *Journal of the Chemical Society, Faraday Transactions 1*, **76**, 314–321.

Chang, F.-R.C., Skipper, N.T. and Sposito, G. (1998) Monte Carlo and molecular dynamics simulations of electrical double-layer structure in potassium-montmorillonite hydrates. *Langmuir*, **14**, 1201–1207.

Chipera, S.J. and Bish, D.L. (2001) Baseline studies of the Clay Minerals Society source clays: Powder X-ray diffraction analyses. *Clays and Clay Minerals*, **49**, 398–409.

Duval, F.P., Porion, P. and Van Damme, H. (1999) Microscale and macroscale diffusion of water in colloidal gels. A pulsed field gradient and NMR imaging investigation. *Journal of Physical Chemistry B*, **103**, 5730–5735.

Duval, F.P., Porion, P., Faugère, A.-M. and Van Damme, H. (2001) An NMR investigation of water self-diffusion and relaxation rates in controlled ionic strength laponite sols and gels. *Journal of Colloid and Interface Science*, **242**, 319–326.

Feinauer, A. and Majer, G. (2001) Diffusion of [23]Na and [39]K in the eutectic melt $Na_{0.32}K_{0.68}$. *Physical Review B*, **64**, 134302.

Fripiat, J.J., Cases, J., Francois, M. and Letellier, M. (1982) Thermodynamic and microdynamic behavior of water in clay suspensions and gels. *Journal of Colloid and Interface Science*, **89**, 378–400.

Fripiat, J.J., Letellier, M. and Levitz, P. (1984) Interaction of water with clay surfaces. *Philosophical Transactions of the Royal Society of London*, **A311**, 287–299.

Furusawa, T. (1997) Synthesis and utilization of clay minerals. *Journal of Clay Science Society of Japan*, **37**, 112–117 (in Japanese with English abstract).

Grandjean, J. and Laszlo, P. (1989) Multinuclear and pulsed gradient magnetic resonance studies of sodium cations and of water reorientation at the interface of a clay. *Journal of Magnetic Resonance*, **83**, 128–137.

Ichikawa, Y., Kawamura, K., Nakano, M., Kitayama, K. and Kawamura, H. (1999) Unified molecular dynamics and homogenization analysis for bentonite behavior: Current results and future possibilities. *Engineering Geology*, **54**, 21–31.

Ichikawa, Y., Kawamura, K., Nakano, M., Kitayama, K., Seiki, T. and Theramast, N. (2001) Seepage and consolidation of bentonite saturated with pure- or salt-water by the method of unified molecular dynamics and homogenization analysis. *Engineering Geology*, **60**, 127–138.

Johnson, C.S., Jr. (1996) Diffusion measurements by magnetic field gradient method. Pp. 1626–1644 in: *Encyclopedia of Nuclear Magnetic Resonance* (D.M. Grant and R.K. Harris, editors). John Wiley & Sons, New York.

Kasama, T., Murakami, T., Kohyama, N. and Watanabe, T. (2001) Experimental mixtures of smectite and rectorite: Reinvestigation of 'fundamental particles' and 'interparticle diffraction'. *American Mineralogist*, **86**, 105–114.

Latour, L.L., Kleinberg, R.L., Mitra, P.P. and Sotak, C.H. (1995) Pore-size distributions and tortuosity in heterogeneous porous media. *Journal of Magnetic Resonance*, **A112**, 83–91.

Mermut, A.R. and Cano, A.F. (2001) Baseline studies of the Clay Minerals Society source clays: Chemical analyses of major elements. *Clays and Clay Minerals*, **49**, 381–386.

Mills, R. (1973) Self-diffusion in normal and heavy water in the range 1–45°. *Journal of Physical Chemistry*, **77**, 685–688.

Monma, T., Kudo, M. and Masuko, T. (1997) Flow behaviors of smectite/water suspensions in terms of particle-coagulated structures. *Journal of the Clay Science Society of Japan*, **37**, 47–57 (in Japanese with English abstract).

Nakashima, Y. (2000) Effects of clay fraction and temperature on the H_2O self-diffusivity in hectorite gel: A pulsed-field-gradient spin-echo nuclear magnetic resonance study. *Clays and Clay Minerals*, **48**, 603–609.

Nakashima, Y. (2001a) Pulsed field gradient proton NMR study of the self-diffusion of H_2O in montmorillonite gel: Effects of temperature and water fraction. *American Mineralogist*, **86**, 132–138.

Nakashima, Y. (2001b) Measurement of the water self-diffusivity in clay gels by nuclear magnetic resonance. *Abstract of the Joint Meeting of Earth and Planetary Science* (http://mc-net.jtbcom.co.jp/earth2001/session/pdf/mm/mm-p002_e.pdf)

Nakashima, Y. (2002a) Effects of the pore size on proton transverse relaxation times: Laboratory experiments for the nuclear magnetic resonance logging. *BUTSURI-TANSA (Geophysical Exploration)*, **55**, 5–18 (in Japanese with English abstract).

Nakashima, Y. (2002b) Self-diffusion of H_2O in stevensite gel: Effects of temperature and clay fraction. *Clay Minerals*, **37**, 83–91.

Nakashima, Y. (2002c) Measurement of H_2O self-diffusion coefficients in clay gels by pulsed-field-gradient nuclear magnetic resonance: A review (in Japanese with English abstract). *Journal of the Clay Science Society of Japan*, **42**, 37–50.

Nakashima, Y. (2002d) Diffusion of H_2O and I^- in expandable mica and montmorillonite gels: Contribution of bound H_2O.

Clays and Clay Minerals, **50**, 1–10.

Nakashima, Y., Mitsumori, F., Nakashima, S., and Takahashi, M. (1999) Measurement of self-diffusion coefficients of water in smectite by stimulated echo ^{1}H nuclear magnetic resonance imaging. *Applied Clay Science*, **14**, 59–68.

Ohtaki, H. and Radnai, T. (1993) Structure and dynamics of hydrated ions. *Chemical Reviews*, **93**, 1157–1204.

Stauffer, D. (1985) *Introduction to Percolation Theory*. Taylor & Francis, London, 124 pp.

Stejskal, E.O. and Tanner, J.E. (1965) Spin diffusion measurements: Spin echos in the presence of a time-dependent field gradient. *Journal of Chemical Physics*, **42**, 288–292.

Suzuki, S., Fujishima, A., Ueno, K., Ichikawa, Y., Kawamura, K., Fujii, N., Shibata M., Sato, H. and Kitayama, K. (2001) Microstructural modeling of compacted sodium-bentonite and application of unified molecular dynamics/homogenization analysis for diffusion process. *Journal of the Clay Science Society of Japan*, **41**, 43–57 (in Japanese with English abstract).

Tokita, M., Miyoshi, T., Takegoshi, K. and Hikichi, K. (1996) Probe diffusion in gels. *Physical Review E*, **53**, 1823–1827.

Watanabe, Y. and Nakashima, Y. (2002) RW3D.m: Three-dimensional random walk program for the calculation of the diffusivities in porous media. *Computers & Geosciences*, **28**, 583–586.

Yong, R.N. (1999) Overview of modeling of clay microstructure and interactions for prediction of waste isolation barrier performance. *Engineering Geology*, **54**, 83–91.

Yu, J.W. and Neretnieks, I. (1997) Diffusion and sorption properties of radionuclides in compacted bentonite. *SKB Technical Report* (Swedish Nuclear Fuel and Waste Management Co.), **97-12**, 1–98.

Zhou, J., Lu, X., Wang, Y. and Shi, J. (2002) Molecular dynamics study on ionic hydration. *Fluid Phase Equilibria*, **194**, 257–270.